Journal of
PERIODONTAL RESEARCH

J Periodont Res 2011; 46: 730–741

JOURNAL OF PERIODONTAL RESEARCH
doi:10.1111/j.1600-0765.2011.01396.x

Reduced functional loads alter the physical characteristics of the bone–periodontal ligament–cementum complex

E. L. Niver[1], N. Leong[2], J. Greene[2], D. Curtis[2], M. I. Ryder[1], S. P. Ho[2]
[1]Division of Periodontology, Department of Orofacial Sciences, University of California San Francisco, San Francisco, CA, USA and [2]Division of Biomaterials and Bioengineering, Department of Preventive and Restorative Dental Sciences, University of California San Francisco, San Francisco, CA, USA

Niver EL, Leong N, Greene J, Curtis D, Ryder MI, Ho SP. Reduced functional loads alter the physical characteristics of the bone–periodontal ligament–cementum complex. J Periodont Res 2011; 46: 730–741. © 2011 John Wiley & Sons A/S

Background and Objective: Adaptive properties of the bone–periodontal ligament–tooth complex have been identified by changing the magnitude of functional loads using small-scale animal models, such as rodents. Reported adaptive responses as a result of lower loads due to softer diet include decreased muscle development, change in structure–function relationship of the cranium, narrowed periodontal ligament space, and changes in the mineral level of the cortical bone and alveolar jaw bone and in the glycosaminoglycans of the alveolar bone. However, the adaptive role of the dynamic bone–periodontal ligament–cementum complex to prolonged reduced loads has not been fully explained to date, especially with regard to concurrent adaptations of bone, periodontal ligament and cementum. Therefore, in the present study, using a rat model, the temporal effect of reduced functional loads on physical characteristics, such as morphology and mechanical properties and the mineral profiles of the bone–periodontal ligament–cementum complex was investigated.

Material and Methods: Two groups of 6-wk-old male Sprague–Dawley rats were fed nutritionally identical food with a stiffness range of 127–158 N/mm for hard pellet or 0.3–0.5 N/mm for soft powder forms. Spatio-temporal adaptation of the bone–periodontal ligament–cementum complex was identified by mapping changes in the following: (i) periodontal ligament collagen orientation and birefringence using polarized light microscopy, bone and cementum adaptation using histochemistry, and bone and cementum morphology using micro-X-ray computed tomography; (ii) mineral profiles of the periodontal ligament–cementum and periodontal ligament–bone interfaces by X-ray attenuation; and (iii) microhardness of bone and cementum by microindentation of specimens at ages 6, 8, 12 and 15 wk.

Results: Reduced functional loads over prolonged time resulted in the following adaptations: (i) altered periodontal ligament orientation and decreased periodontal ligament collagen birefringence, indicating decreased periodontal ligament turnover rate and decreased apical cementum resorption; (ii) a gradual increase in X-ray attenuation, owing to mineral differences, at the periodontal ligament–bone and periodontal ligament–cementum interfaces, without significant differences in the gradients for either group; (iii) significantly ($p < 0.05$) lower microhardness of alveolar bone (0.93 ± 0.16 GPa) and secondary cementum (0.803 ± 0.13 GPa) compared with the higher load group insert bone = (1.10 ± 0.17 and cementum = 0.940 ± 0.15 GPa, respectively) at 15 wk, indicating a temporal effect of loads on the local mineralization of bone and cementum.

Conclusion: Based on the results from this study, the effect of reduced functional loads for a prolonged time could differentially affect morphology, mechanical properties and mineral variations of the local load-bearing sites in the bone–periodontal ligament–cementum complex. These observed local changes in turn could help to explain the overall biomechanical function and adaptations of the tooth–bone joint. From a clinical translation perspective, our study provides an insight into modulation of load on the complex for improved tooth function during periodontal disease and/or orthodontic and prosthodontic treatments.

Sunita P. Ho, PhD, Division of Biomaterials and Bioengineering, Department of Preventive and Restorative Dental Sciences, 707 Parnassus, D 2252, University of California San Francisco, San Francisco, CA 94143, USA
Tel: +1 415 514 2818
Fax: +1 415 476 0858
e-mail: sunita.ho@ucsf.edu

Key words: functional load; tissue interface; cementum; bone–tooth biomechanics; alveolar bone; periodontal ligament

Accepted for publication June 14, 2011

Mechanical loads are important in maintaining joint function (1). In the masticatory system, functional loads on a bone–tooth fibrous joint (2) are enabled by the muscles of mastication, including the masseter, temporalis, medial pterygoid and upper/lower lateral pterygoid (3). Magnitudes and frequencies of functional loads are dependent on many intrinsic and extrinsic factors (4), including muscle efficiency (e.g. higher in men than in women, higher in younger than in older; 5–7), hardness of diet (e.g. softer foods and/or liquid diet vs. harder foods; 8–10) and other forms of habitual loads (e.g. nail biting, tongue thrusting, jaw clenching, bruxism; 11–13). As a result, functional loads cause a combination of axial and horizontal loads, resulting in tooth movement in all directions relative to the alveolar bone (5,14). Hence, it is conceivable that a change in magnitude of functional loads due to any or a combination of the aforementioned factors can change the axial and lateral loads on a tooth and its relative position within the alveolar socket.

The unique anatomy of the bone–tooth joint features two different hard tissues, cementum and alveolar bone, attached by the fibrous periodontal ligament (2). Cementum is a mineralized composite of fibrillar and nonfibrillar proteins (organic range of 45–60%) and inorganic apatite (inorganic range of 40–55%) with a lamellar-like structure (15). Alveolar bone has similar ranges of organic and inorganic contents, but the structure of the extracellular matrix is different from cementum. Alveolar bone is vascularized, and goes through physiological remodeling and a significant response to mechanical loads identified as modeling of bone (16,17). Attached to the cementum and bone is the vascularized and innervated periodontal ligament, which is critically important in adaptive responses and is responsible for tooth movement relative to the alveolar socket and resulting strain fields within the bone–periodontal ligament–cementum complex. Unlike diarthroidal joints of the musculoskeletal system (18), the bone–tooth fibrous joint has a limited range of motion (19) during function. Within the bone–periodontal ligament–cementum complex, bone, cementum, periodontal ligament, periodontal ligament–bone and periodontal ligament–cementum attachment sites, and the interfaces between soft (periodontal ligament) and hard tissues (bone and cementum, i.e. both primary and secondary cementum) jointly serve the common function of mechanical stress dissipation (20) caused by dynamic loads. Over time, tissues, soft–hard tissue attachment sites and interfaces adapt to loads in ways identifiable by changes in physical and chemical properties, resulting in morphologically unique dental organs (16,17).

Following development, functional loads on the bone–tooth complex cause predominant strain fields in the periodontal ligament and stress fields that are more pronounced in bone and cementum (21). Strains within the periodontal ligament and at the periodontal ligament–bone and periodontal ligament–cementum attachment sites (entheses) initiate many of the local adaptive responses of the complex. Hierarchical mapping of cell, tissue and organ responses to biomechanical function will provide an improved basis for understanding and explaining many of the controversies in clinical dentistry.

Functional adaptations (overload, disuse and directional loads) in bone, cementum and the periodontal ligament are often evaluated with systematic studies using small-scale animal models, such as rodents (22). For over 30 years (22–24), tissues of the rat bone–periodontal ligament–cementum complex have been used to investigate load-mediated adaptation. Adaptive properties of the bone–periodontal ligament–tooth complex have been identified by changing the magnitude of functional loads using the following models: hypo- and hyperocclusion (25,26), unopposed teeth (27), orthodontic forces (28), and soft and hard diets (22). Reported adaptive responses as a result of lower loads due to softer diet include decreased muscle development (29,30), a change in the structure–function relationship of the cranium, narrowed periodontal ligament space (31), changes in the mineral level of the cortical bone and alveolar jaw bone (32,33), and changes in the glycosaminoglycan (32) content of alveolar bone. However, the adaptive role of the dynamic bone–periodontal ligament–cementum complex due to prolonged reduced loads has not been fully explained to date, especially with regard to concurrent adaptations of bone, periodontal ligament and cementum. In the present study, it is hypothesized that prolonged functional loads will change the local physical characteristics of the bone–tooth complex. Hence, our objectives were to identify changes in the following: (i) periodontal ligament birefringence and orientation using polarized light microscopy coupled with picrosirius red staining; (ii) adaptive responses by mapping resorptive patterns of cementum and reversal lines in alveolar bone; and (iii) mineral gradients at the bone–periodontal ligament and cementum–periodontal ligament attachment sites using micro-X-ray computed tomography (micro-XCT); and (iv) changes in mechanical hardness of cementum and bone using microindentation in specimens harvested from rats subjected to soft and hard diets for a prolonged time.

Material and methods

Animals and experimental diet

Fifty-six 6-wk-old male Sprague–Dawley rats were obtained from Charles River Laboratories (Wilmington, MA, USA) and housed at University of California San Francisco (UCSF) Animal Facilities. Animal housing, care and with euthanasia protocol complied with the guidelines of the Institutional Animal Care and Use Committee of UCSF and the National Institutes of Health. Rats were randomly allocated to higher (n = 32) or lowerfunctional load groups (n = 24) by feeding them nutritionally identical food (PicoLab 5058, LabDiet, Dean's Animal Feeds, Redwood City, CA, USA), in either a hard pellet or soft powder food form. The rats were allowed food and water *ad libitum*. At the zero time point (age 6 wk), considered as baseline, eight rats were killed as control animals, and by default belonged to the higher functional load group because they are normally fed hard pellets after being weaned. At subsequent time points of 8, 12 and 15 wk, eight rats from each group were killed, and their mandibles immediately harvested for specimen preparation.

Food stiffness

Compression tests were conducted using a mechanical testing device (Fig. 1A; Bose Electrofoce 3200 system; EnduraTec, Minnetonka, MN, USA) and by individually loading hard pellets (Fig. 1B) and bulk soft powder (Fig. 1C). Soft food was loaded at a rate of 0.1 mm/s to an average maximal displacement of 5.52 mm. Soft food was loaded at a faster rate to prevent discrepancies due to particle disbursement within the container. Student's unpaired t-test with 95% confidence intervals indicated significant differences in mean stiffness (p < 0.05) of hard food at 150 ± 15 N/mm compared with soft food at 0.4 ± 0.1 N/mm.

Histology

Half of the left mandibles from each group at each time point (n = 4) were fixed in formalin, demineralized in Immunocal (Decal Chemical Corporation, Tallman, NY, USA), then embedded in paraffin, from which 5- to 6-μm-thick sections were taken and mounted, deparaffinized with xylene, and stained with either hematoxylin and eosin (H&E) or picrosirius red. The stained tissues were characterized for structural orientation and integration of the periodontal ligament with bone and cementum, using a light microscope (BX 51; Olympus America Inc., San Diego, CA, USA) and analyzed using Image Pro Plus v6.0 software (Media Cybernetics Inc., Silver Springs, MD, USA).

Micro-X-ray computed tomography (Micro XCT)

The left mandibles (n = 4) from each group at each time point were fixed and imaged in 70% ethanol. Each specimen was scanned (Micro XCT-200; Xradia Inc., Pleasanton, CA, USA) with identical experimental parameters (75 kVp, 6 W at ×4 magnification), then reconstructed (Fig. 2A) and viewed with identical contrast and brightness settings. Virtual parallel slices (from tomographies) were used to bisect the distal root of the second mandibular molar (see also Supporting Information) by indentifying the apical orifice as a landmark. Additionally, transverse sections of the distal root of the second molar (Fig. 2D) for each specimen were analyzed using ImageJ (http://rsb.info.nih.gov/ij/). The X-ray attenuation of alveolar bone and cementum as a function of distance from the periodontal ligament space after normalizing intensity values within each specimen was plotted using MATLAB® R2008a (MathWorks®, El Segundo, CA, USA). Measurements were made using transverse sections (Fig. 2) to avoid cortical bone and endosteal and/or other vascular spaces and were limited to 80 μm in bone and cementum, respectively.

Ultrasectioning of specimens and microindentation

The molar portions from the right mandibles of each group at each time point (n = 4) were first sectioned to isolate the distal root of the second molar (see also Supporting Information), and then glued to atomic force microscope steel stubs (Ted Pella, Inc., Redding, CA, USA) using epoxy resin. A diamond knife (MicroStar Technologies, Huntsville, TX, USA) was used to perform final sectioning by removing 300-nm-thick sections (34). The sectioned surface of the remaining block was characterized for primary cementum, secondary cementum and alveolar bone using a light microscope.

Microhardness values of bone and cementum were evaluated to distinguish significant influences of loading over time. Microindentation on mineralized tissues using ultrasectioned blocks (n = 4) was performed in dry conditions with the use of a microindenter (Buehler Ltd, Lake Bluff, IL, USA) and a Knoop diamond indenter (Buehler Ltd) at 10gf. Each specimen

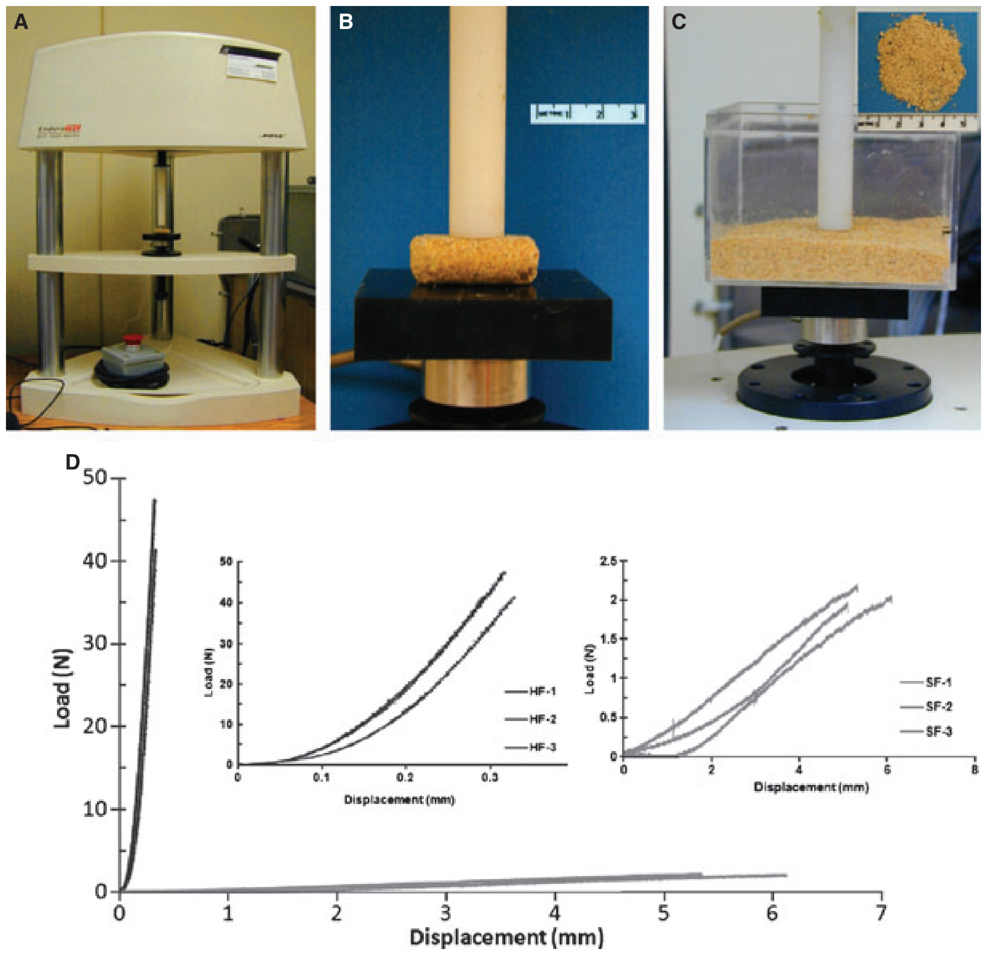

Fig. 1. (A) Compression testing system. (B) Individual unconfined hard pellets were loaded in compression to determine the stiffness of the hard food. (C) Powdered soft food was confined within a hard plastic container and compressively loaded to determine the stiffness of the soft food. (D) The stiffness of the hard food (HF 1–3) and soft food (SF 1–3) was determined by the slope of the linear portion of the load vs. displacement curve. Mean stiffness of hard food, 150 ± 15 N/mm; and soft food, 0.4 ± 0.1 N/mm.

was indented in cementum and bone, and the distance between any two indents was chosen per American Standard for Testing Materials standard (35). Statistically significant differences between groups were determined using Student's unpaired *t*-test with a 95% confidence interval.

Results

Periodontal ligament collagen fiber organization

Polarized light microscopy of picrosirius red stained sections of the distal root of the second molar (M2/D) revealed distinct differences between periodontal ligament collagen fibers with lower loads compared with higher loads (Fig. 3). Periodontal ligament collagen fibers subjected to lower loads were birefringent (Fig. 3A and B), but were disorganized, with lower intensity, and patchy appearance. Periodontal ligament collagen fibers subjected to higher loads demonstrated a strong birefringence (Fig. 3C and 3D) and were well oriented and organized.

Regional cementum resorption patterns and bone modeling activity

Three-dimensional reconstructions of the distal root of molar two (M2/D) region subjected to lower and higher loads demonstrated regional pitting on the distal root surface, a characteristic of resorption activity at the periodontal ligament–cementum attachment site. A representative two-dimensional slice of M2/D shown in Fig. 4A illustrates the affected regions, as follows: the coronal region (CR) in primary cementum; the mid-root region (MR), spanning the transition between primary and secondary cementum; and the apical region (AR), with only secondary cementum. Extensive resorption was observed in the CR and MR (Fig. 4B) at all time points in rats subjected to lower loads. Apposition of secondary cementum is seen with age, as expected, in both groups, but cementum resorption in the AR decreased over time in rats subjected to lower loads.

In rats subjected to higher loads (Fig. 4C), the distribution of cementum

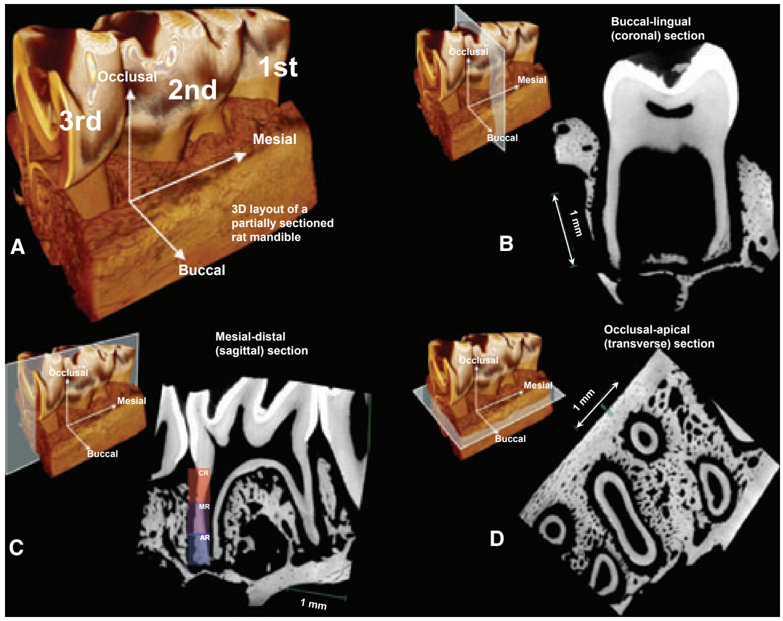

Fig. 2. (A) Three-dimensional (3D) reconstruction of mandibular molar region. (B–D) Reconstructed two-dimensional slices representing coronal, middle and apical regions, buccal–lingual (B), mesial–distal (C) and occusal–apical planes (D), respectively. The coronal region (CR), all primary cementum, is shown in red, the mid-root region (MR), spanning the interface of the primary and secondary cementum, in purple, and the apical region (AR), all secondary cementum, in blue. Scale bars represent 1 mm.

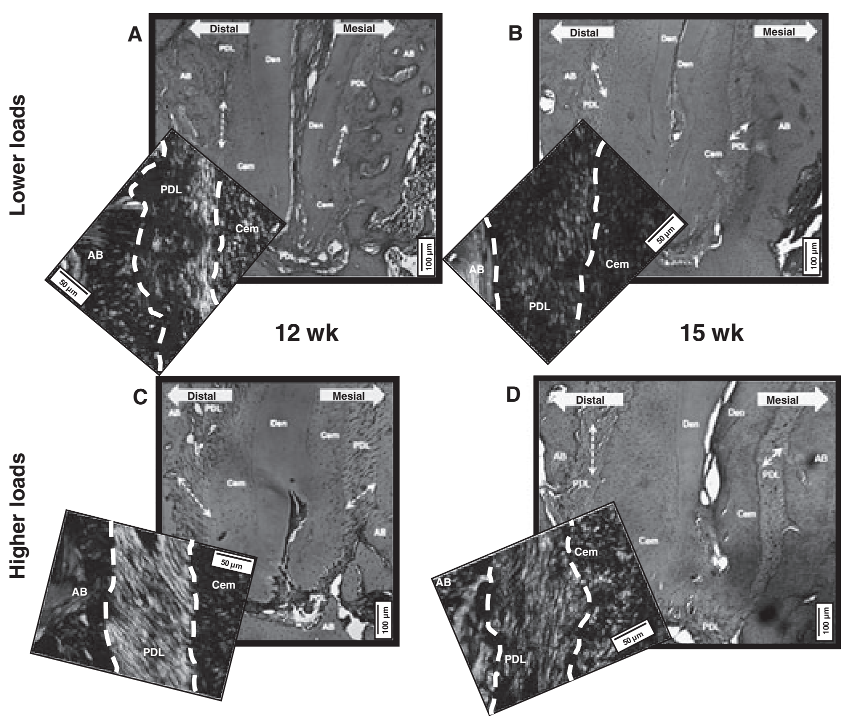

Fig. 3. Light microscope images of the distal root of molar two (M2/D) stained with hematoxylin and eosin at ×10 magnification to illustrate the variations in periodontal ligament (PDL) orientation. Representative insets of polarized light micrographs of picosirius red stained of a picrosirius red stained bone–PDL–cementum attachment site of M2/D at ×40 magnification. (A,B) The M2/D subjected to lower loads illustrates less organized PDL collagen fibrils, with patchy and dim PDL birefringence. (C,D) The M2/D subjected to higher loads illustrates organized PDL collagen fibrils, with a distinct and bright appearance of the PDL. Abbreviations: AB, alveolar bone; Cem, cementum; Den, dentin; PDL, periodontal ligament. Scale bars represent 100 µm; inset scale bars represent 50 µm.

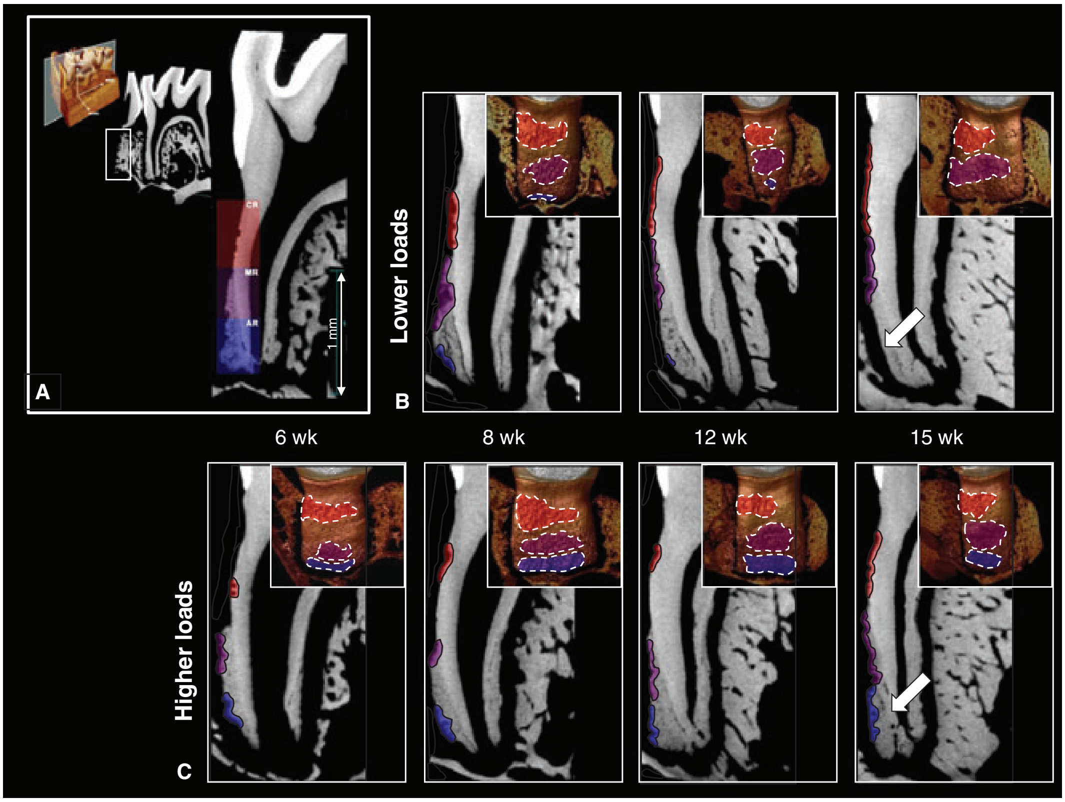

Fig. 4. (A) Representative resorption sites on a mesial–distal two-dimensional slice of a mandibular second molar. Areas of resorption are colored in both mesial–distal two-dimensional reconstructed slices and corresponding tomographs for all groups. Extensive resorption can be observed in the coronal region (CR) and mid-root region (MR) for all groups. However, in the lower functional load groups (B) there is little or no resorption in the apical region (AR) compared with the higher functional load groups (C; white arrows).

resorption in the CR and MR was similar to those subjected to lower loads at all time points. Also, secondary cementum apposition occurred with age. However, with prolonged time a marked increase in areas of secondary cementum resorption in the AR was observed in teeth loaded with higher functional loads compared with teeth loaded with lower functional loads (areas of secondary cementum resorption patterns highlighted in Fig. 4).

Analysis of hematoxylin and eosin stained light micrographs of M2/D illustrated a distribution of reversal lines (Fig. 5) corresponding to regional patterns of cementum resorption identified in Fig. 4. In rats subjected to lower loads (Fig. 5B), reversal lines in bone increased with time, especially in the CR opposing areas of primary cementum resorption. In contrast, rats subjected to higher loads (Fig. 5C) showed an increase in reversal lines in bone with time, but predominantly in the AR opposing areas of secondary cementum resorption.

Mineral gradients at the periodontal ligament–bone and periodontal ligament–cementum interfaces

Two-dimensional reconstructed slices of the M2/D region revealed gradients in X-ray attenuation at the periodontal ligament–bone interface and at the periodontal ligament–cementum interface, with nearly constant values of attenuation in bone and cementum, respectively, for both lower and higher loads at all time points (Fig. 6). The results in Fig. 6 illustrate that the first 25 μm near the periodontal ligament–bone (Fig. 6B and E) and first 15 μm near the periodontal ligament–cementum attachment sites (Fig. 6C and F) are less mineralized than the respective bulk tissues. Although no significant differences were observed, X-ray attenuation was lower in bone and cementum subjected to lower loads (Fig. 6B and C) than in respective tissues subjected to higher loads (Fig. 6E and F; note the scale bars for respective plots; Fig. 6E and F share the same scale bar).

Mechanical properties of bulk secondary cementum and bone

Knoop hardness of cementum increased from 0.51 ± 0.11 GPa at 6 wk (baseline) to 0.94 ± 0.15 GPa at 15 wk, while in the lower load group the hardness increased to 0.80 ± 0.13 GPa at 15 wk (Fig. 7A). Additionally, cementum subjected to higher loads was significantly harder ($p < 0.05$) at 12 (0.90 ± 0.15 GPa) and 15 wk (0.94 ± 0.15 GPa) compared to those at lower loads (0.78 ± 0.15 and 0.80 ± 0.13 GPa, respectively; Fig. 7A).

Knoop hardness of bone increased from 0.64 ± 0.14 GPa at 6 wk (baseline) to 1.1 ± 0.17 GPa at 15 wk,

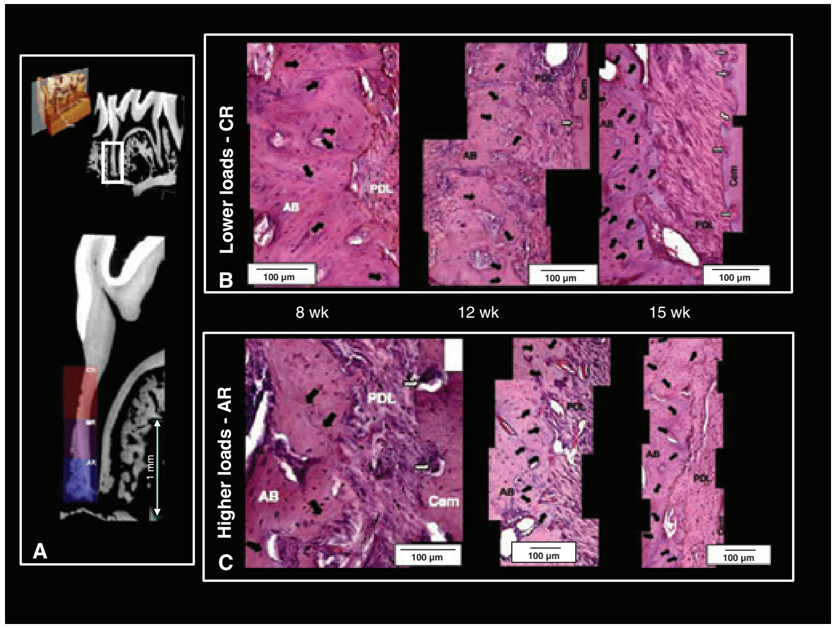

Fig. 5. (A) Representative tomograph and two-dimensional sagittal section illustrating the examined regions of the bone–PDL–cementum complex subjected to lower (B) and higher loads (C). (B,C) Light micrographs of the distal root of molar two at ×20 magnification illustrating variations in reversal lines (black lines) in alveolar bone. (B) Reversal lines increase with age in the coronal region (CR) opposing areas of primary cementum resorption (white arrows). (C) Reversal lines increase with age in the apical region (AR) opposing areas of secondary cementum resorption (white arrows). Abbreviations: AB, alveolar bone; Cem, cementum; PDL, periodontal ligament. Scale bars represent 100 µm.

while in the lower load group the hardness increased to 0.93 ± 0.16 GPa at 15 wk (Fig. 7B). Bone subjected to higher loads was significantly harder ($p < 0.05$) at the 12 (1.0 ± 0.19 GPa) and 15 wk time points (1.1 ± 0.17 GPa) than when subjected to lower loads (0.89 ± 0.18 and 0.93 ± 0.16 GPa, respectively; Fig. 7B).

Discussion

In this study, functional loads were modulated by changing the hardness of the food (8,29,30); a hard pellet diet with a higher compressive strength was compared with a soft powdered diet with negligible compressive strength (Fig. 1). Consequently, rats on a hard pellet diet experienced higher functional loads, while those fed a soft powdered diet experienced lower functional loads (Fig. 1) (22,36). Subsequently, adaptation to higher and lower loads was investigated by spatial (CR, MR and AR; Fig. 2) and temporal mapping (6, 8, 12 and 15 wk) of changes in physical and chemical properties. The chain of events leading to the observed adaptation in the complex at these three potential load-bearing sites can be explained as follows. The decreased magnitude of functional load from a soft diet with a compressive strength of 0.3–0.5 N/mm could decrease periodontal ligament collagen turnover rate due to decreased tooth movement relative to bone (37,38). A decrease and/or loss of occlusal function resulted in atrophy of the periodontal ligament and was related to a loss of lower and higher molecular weight proteoglycans responsible for the structural maintenance and mechanical integrity of the periodontal ligament (39–48). The innervated periodontal ligament contains vasculature, various types of collagen (including types I, III, V, VI and XII) and several noncollagenous proteins that contribute to the chemically bound fluid, maintenance of hydrostatic pressure, load regulation and dissipation, and provision of nutrients (49,50). However, the innate birefringence of the periodontal ligament decreases significantly when the molecular structure of collagen is degraded as a result of decreased turnover due to inadequate loading (51–53). In the present study, a strong periodontal ligament birefringence was observed at all three anatomical locations of the complex subjected to higher loads (Fig. 3C and D) and what are considered to be normal functional loads for a rat, while a patchy, diffuse birefringence was observed in periodontal ligament subjected to lower functional loads (Fig. 3A and B). Fundamentally, enhancement of birefringence can only be observed when sirius red molecules are bound to oriented, highly organized collagen molecules (54). Hence, aberrations to functional loads can change the physiological program within periodontal ligament cells, altering the biochemical events and the structural and mechanical integrity of the periodontal ligament matrix, thereby redefining the local events in the complex, as observed in this study.

The current dogma states that the acellular primary cementum is responsible for tooth attachment, while apical and cellular secondary cementum is responsible for resisting functional loads (19). However, the observed local changes in coronal and apical cementum and in the corresponding

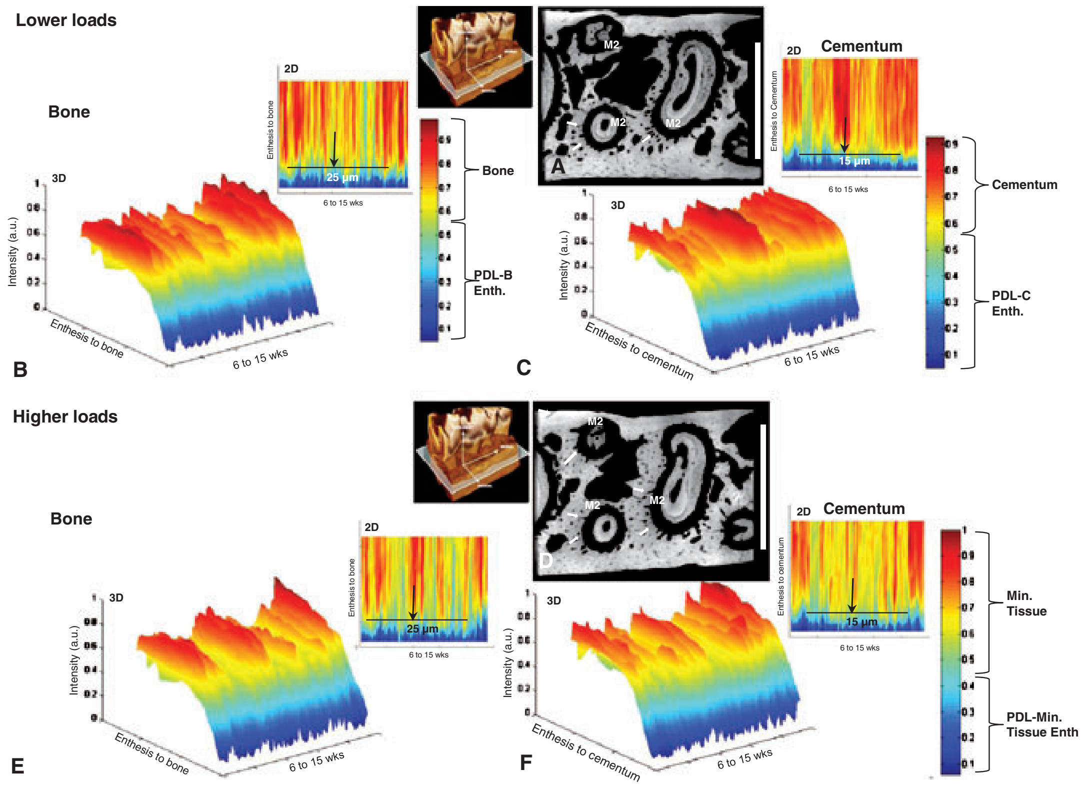

Fig. 6. (A,D) Transverse sections illustrating trailing and leading envelopes of the tooth as darker and lighter attenuating regions (white arrows). Bone–tooth complex was subjected to lower loads (A) and higher loads (D). X-ray intensity profiles illustrate gradients (normalized) due to mineral variation in alveolar bone near the periodontal ligament (PDL)–bone interface, and PDL–cementum interface of secondary cementum for lower (B,C) and higher functional loads (E,F) at all time points in bone and secondary cementum. Note that the 6 wk higher load group is also shown in the lower load for ease of comparison. For all time points and locations, the intensity gradually increases in the first 25 μm (for bone) or 15 μm (for cementum) from the PDL space into mineralized tissue, with no significant differences between the higher and lower load groups. An apparent decrease in X-ray attenuation in bone and cementum subjected to lower loads (B,C) compared with higher loads (E,F) was observed. Abbreviations: M2, molar 2; PDL-Min. Tissue Enth., enthesis of PDL-respective mineralized tissue.

bone and periodontal ligament could be considered as necessary adaptive responses to preserve the functional mechanics of the bone–tooth joint. These adapted sites can also be noted as local load-bearing sites within the bone–periodontal ligament–cementum complex of molars. The strains in the local load-bearing sites of the bone–periodontal ligament–tooth complex are often broadly categorized as tensile and compressive strains due to widening and narrowing of the periodontal ligament space within the complex. While this is true, other areas, such as the endosteal and trabecular spaces within the alveolar process, are also stimulated by flow of interstitial fluid caused by functional loads. In the present study, as lower loads decreased tooth mobility and periodontal ligament strain, resulting in a loss of periodontal ligament mechanical integrity, it can be hypothesized that the mechanobiological events prompted by integrin-based cell–matrix and cell-cell interactions at the periodontal ligament–cementum and periodontal ligament–bone attachment sites were altered (49), resulting in resorption of the bone and primary cementum of the distal root. This observation was consistent, but to a lesser degree within the complex subjected to higher loads. Rather, higher loads transmit greater force to the apical region of the root, and as a result increased secondary cementum resorption was observed. While secondary cementum resorption in teeth subjected to lower loads was observed at earlier time points, the amount of resorption decreased over time (Fig. 4B), indicating the adaptive effects of the reduced functional loads apically on the complex. Over time, reduced functional loads suppress activity of the masticatory muscles, decrease load across the facial skeleton (29), diminish apically directed compressive forces (55), and result in decreased secondary cementum resorption. This observation was consistent with models that illustrated a significant increase in secondary cementum with a decrease/absence of functional loads (24,56).

In the present study, resorption sites were consistently observed in the coronal, middle and apical regions of the distal side of M2/D in 6-wk-old rats, probably due to innate distal drift as mentioned by others (24,27, 57). However, when subjected to lower loads over time, the degree of resorption and resorption patterns were

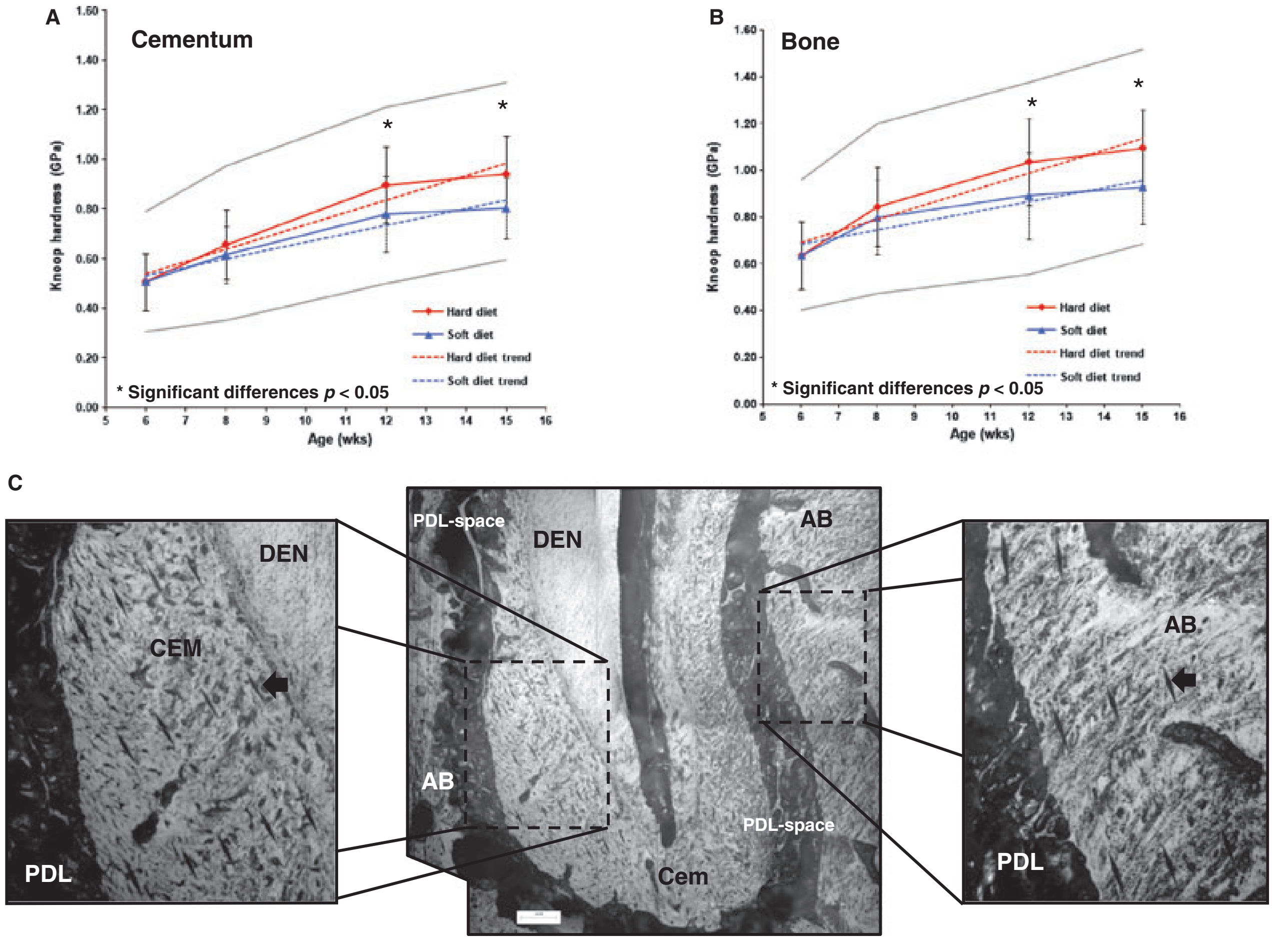

Fig. 7. (A) Mean hardness values of alveolar bone for higher and lower load groups at each time point. (B) Mean hardness values of secondary cementum determined by microindentation for higher and lower load groups at each time point. Ranges of hardness values are represented by gray lines above (maximum) and below (minimum). At all experimental time points (8, 12 and 15 wk), respective bone and cementum hardness values in the higher load group were greater than in the lower load group. Asterisks indicate statistical significance ($p < 0.05$) between groups at the 12 and 15 wk time points. (C) Light microscope images illustrate microindents in alveolar bone (AB) and secondary cementum (CEM) (black arrows). PDL, periodontal ligament; DEN, dentin. Scale bar represents 100 μm.

altered at the load-bearing sites. On the opposing side formed by bone, higher loads could have resulted in increased hydrostatic pressure within the endosteal and trabecular spaces (51,52), resulting in adaptation of bone identified by reversal lines (Fig. 5). At later time points, fewer changes in shape were observed in complexes subjected to lower loads (Figs 4 and 5). These observations were similar to those reported by others on skeletal bone and alveolar bone (51,52,58–62).

Distal drift in rats could result in lower and higher X-ray attenuating areas due to trailing and leading envelopes in adapting bone around the tooth (Fig. 5). Although the trailing and leading edge effects are distinct in bone subjected to higher functional loads, they were less evident in bone subjected to lower loads in this study. The complex geometry of the tooth within the alveolar socket, along with the trailing and leading envelopes due to distal drift, could manifest into varying mineral gradients (Fig. 6) due to bone growth on the mesial side and bone resorption on the distal side, thus maintaining a uniform periodontal ligament space at any time point.

Physical and chemical gradients are natural and exist between periodontal ligament and bone and between periodontal ligament and cementum to optimally distribute functional loads (63). As a result of functional loads, the periodontal ligament continues to experience tensile and compressive strains within and at its attachment sites with bone and cementum (21). The varying strains in turn modulate the biochemical expressions through site-specific cells, which act as transducers (i.e. strain gauges) to either increase or decrease expression of biomolecules responsible for apposition or resorption of mineral in bone and cementum. However, no significant differences in intensity were observed in the mineral gradient at the periodontal ligament–bone and periodontal ligament–cementum interface sites (Fig. 6), although higher attenuation of X-rays in cementum and bone subjected to higher loads (Fig. 6B and 6C)

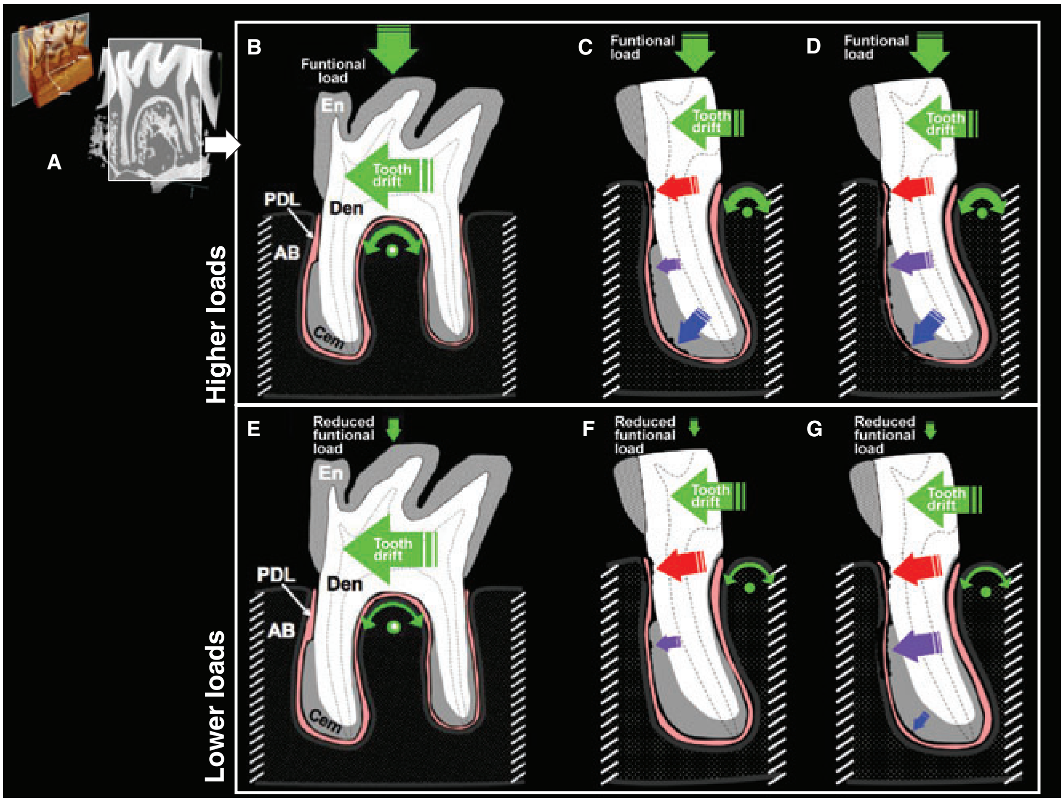

Fig. 8. (A) Virtual slice of molar two taken from a tomograph illustrating the bone–periodontal ligament (PDL)–tooth complex. Schematic diagram of a biomechanical model illustrating dominant forces on the second mandibular rat molar and resulting load-mediated adaptation of tissues in the complex subjected to higher and lower functional loads. (B) The hard pellet diet provides a high functional load and apically directed forces in addition to the distally directed forces due to innate tooth drift. Together, these forces cause the tooth to rotate, with the inter-radicular bone as the fulcrum point (green dot). (C,D) The rotation redirects the apical and distal forces, causing PDL compression between the alveolar bone and the tooth and resulting resorption in the coronal, midroot and apical regions with time. (E) The soft, powdered diet decreases the functional load so that the distally directed forces of tooth drift dictate tooth movement. The anatomy of the inter-radicular bone also creates a fulcrum point (green dot) about which some rotational movement could exist. (F) The distal tooth drift together with some rotation causes regional PDL compression between the alveolar bone and the coronal portion of the tooth, resulting in resorption. (G) In the absence of substantive functional loading, the rotational force on the tooth is minimized, and little compressive force acts on the apical portion of the root. Meanwhile, subsequent tooth drift acts to translate the tooth distally, causing regional PDL compression between the alveolar bone and the tooth in the coronal and midroot regions. Abbreviations: AB, alveolar bone; Cem, secondary cementum; Den, dentin; En, enamel; PDL, periodontal ligament.

was observed. Some possible explanations for these observed effects are as follows: (i) the organic scaffold upon which mineralization occurred was better maintained in the complex that was normally loaded (51,52); (ii) the lower magnification at which the mineral changes were documented was accurate only for macro-scale events, and not sensitive to the micro-scale events within the mineralized tissues; (iii) in order to compare the gradient in cementum to that in bone, equal and limited distances of only 80 μm from the periodontal ligament attachment site into the respective hard tissues were measured; and (iv) the reduction in functional loads could have a moderate effect on bone and cementum mineral concentrations and may be confirmed by extending the study to later time points. Regardless, from a materials and mechanics perspective, the locally identified gradual increase in mineral at the periodontal ligament–bone and periodontal ligament–cementum interfaces could be to accommodate changes in functional loads. The combined effect of the aforementioned loss of periodontal ligament structural integrity and decreased distal drift of rat molars subjected to reduced functional loads could explain the decreased apical resorption and the decreased X-ray attenuation in bone and cementum.

The increasing trend in X-ray attenuation can be related to the increase in the hardness values (Fig. 7) of cementum and bone observed with age in both groups. During development, an increase in hardness with age is expected within groups, but the significant increase in hardness between groups at the 12 and 15 wk time points can be related to the increase in X-ray attenuation and maintenance of the 'quality' of bone and cementum. Functional mineralization is best understood by accounting for the interaction of mineral inside and outside the collagen fibrils that form the tissue scaffold (64,65). However, a compromised mineral–

collagen interaction commonly observed in inadequately loaded mineralized tissue could impair the overall 'quality' of the mineralized tissue (51,66). This could explain the significantly greater hardness (Fig. 7) of bone and cementum subjected to higher loads when compared with inadequately loaded bone and cementum.

This study documents a specific adaptive mechanism of the complex (a reservoir of multiple cell types), originally accustomed to higher loads, and suddenly 'forced' to accommodate reduced loads, which has not been previously shown by others. To summarize with a biomechanical model (Fig. 8), the reduced functional loads can cause a decrease in tooth rotation and lateral loads, and different stress states within the complex. As with any multirooted tooth, the molar could pivot or rotate using the inter-radicular bone as a fulcrum (67) and alter localized widening and narrowing of the periodontal ligament space. This in turn could result in altered tensile and compressive strains of the periodontal ligament, and varying strain gradients at the periodontal ligament–bone and periodontal ligament–cementum attachment sites. Furthermore, the effects of reduced loads are more evident with time, with distinct changes in resorption and mineralization patterns in the 12 and 15 wk groups (Figs 4 and 5). These results can be considered as necessary local adaptations of the complex to accommodate decreased functional loads and to maintain the functional efficiency.

Conclusions

In conclusion, the consistency of the diet affects the functional loads experienced within the tissues of the bone–tooth joint. Lower forces may not be sufficient to maintain tissue homeostasis, and could degrade collagen in the periodontal ligament, alter the distribution of stress-induced resorption, and result in lower 'quality' bone and cementum. From the perspective of clinical translation, this study provides insights into the modulation of load on the complex for improved tooth function during periodontal disease and/or orthodontic and prosthodontic treatments.

Acknowledgements

The authors thank Dr Peter Sargent, Department of Cell and Tissue Biology, for the use of the ultramicrotome. Financial support was provided by Benjamin Dienstein Research Fund, UCSF; NIH/NIDCR R00 DE018212 (SPH), NIH/NCRR 1S10RR026645-01 (SPH); Strategic Opportunities Support (SOS) and T1 Catalyst Clinical and Translational Science Institute (CTSI) University of California (SPH), Departments of Preventive and Restorative Dental Sciences and Orofacial Sciences, UCSF.

Supporting Information

Additional Supporting Information may be found in the online version of this article:

Data S1 1) innate root resorption in rats, and 2) why the 2nd molar offers to be an appropriate biomechanical model.

Please note: Wiley-Blackwell are not responsible for the content or functionality of any supporting materials supplied by the authors. Any queries (other than missing material) should be directed to the corresponding author for the article.

References

1. Carter DR, Beaupre GS. *Skeletal Function and Form*. Cambridge: Cambridge University Press, 2001.
2. Nanci A, Bosshardt DD. Structure of periodontal tissues in health and disease. *Periodontol 2000* 2006;**40:**11–28.
3. Ten Cate AR. *Oral Histology Development, Structure, and Function*, 5th edition. St. Louis: Mosby Year Book Inc., 1998.
4. Woda A, Foster K, Mishellany A, Peyron MA. Adaptation of healthy mastication to factors pertaining to the individual or to the food. *Physiol Behav* 2006;**89:**28–35.
5. Graf H. *Occlusal Forces and Mandibular Movements*. Elmsford, NY: Pergamon Press, Inc., 1978.
6. Graf H. A method for measurement of occlusal forces in three directions. *Helv Odontol Acta* 1974;**18:**7–11.
7. Graf H. *Occlusal Forces During Function*. Ann Arbor, Michigan: University of Michigan Press, 1975.
8. Sako N, Okamoto K, Mori T, Yamamoto T. The hardness of food plays an important role in food selection behavior in rats. *Behav Brain Res* 2002;**133:**377–382.
9. Grunheid T, Langenbach GE, Brugman P, Everts V, Zentner A. The masticatory system under varying functional load. Part 2: effect of reduced masticatory load on the degree and distribution of mineralization in the rabbit mandible. *Eur J Orthod* 2010;1–7.
10. Vreeke M, Langenbach GE, Korfage JA, Zentner A, Grunheid T. The masticatory system under varying functional load. Part 1: structural adaptation of rabbit jaw muscles to reduced masticatory load. *Eur J Orthod* 2010;1–6.
11. Hartsfield JK Jr. Pathways in external apical root resorption associated with orthodontia. *Orthod Craniofac Res* 2009;**12:** 236–242.
12. Hartsfield JK Jr, Everett ET, Al-Qawasmi RA. Genetic factors in external apical root resorption and orthodontic treatment. *Crit Rev Oral Biol Med* 2004;**15:**115–122.
13. Rugh JD, Harlan J. Nocturnal bruxism and temporomandibular disorders. *Adv Neurol* 1988;**49:**329–341.
14. Picton DCA. Titling movements of teeth during biting. *Arch Oral Biol* 1962;**7:**151–159.
15. Bosshardt DD, Selvig KA. Dental cementum: the dynamic tissue covering of the root. *Periodontol 2000* 1997;**13:**41–75.
16. Saffar JL, Lasfargues JJ, Cherruau M. Alveolar bone and the alveolar process: the socket that is never stable. *Periodontol 2000* 1997;**13:**76–90.
17. Frost HM. Wolff's Law and bone's structural adaptations to mechanical usage: an overview for clinicians. *Angle Orthod* 1994;**64:**175–188.
18. Blau PJ, Lawn BR, American Society for Testing and Materials, Committee E-4 on Metallography, International Metallographic Society. *Microindentation Techniques in Materials Science And Engineering: A Symposium Sponsored by ASTM Committee E-4 on Metallography and by the International Metallographic Society, Philadelphia, PA, 15–18 July 1984*. Philadelphia, PA: International Metallographic Society, 1986:303.
19. Nanci A. *Ten Cate*'s Oral Histology: Development, Structure, and Function, 6th edition. Saint Louis: Mosby, 2003.
20. Benjamin M, Toumi H, Ralphs JR, Bydder G, Best TM, Milz S. Where tendons and ligaments meet bone: attachment sites ('entheses') in relation to exercise and/or mechanical load. *J Anat* 2006;**208:**471–490.

21. Qian L, Todo M, Morita Y, Matsushita Y, Koyano K. Deformation analysis of the periodontium considering the viscoelasticity of the periodontal ligament. *Dent Mater* 2009;**25:**1285–1292.
22. Hiiemae K. Mechanisms of food reduction, transport and deglutition: how the texture of food affects feeding behavior. *J Texture Stud* 2004;**35:**171–200.
23. Hiiemae KM. Masticatory function in the mammals. *J Dent Res* 1967;**46:**883–893.
24. Schneider BJ, Meyer J. Experimental studies on the interrelations of condylar growth and alveolar bone formation. *Angle Orthod* 1965;**35:**187–199.
25. Ohshima S, Komatsu K, Yamane A, Chiba M. Prolonged effects of hypofunction on the mechanical strength of the periodontal ligament in rat mandibular molars. *Arch Oral Biol* 1991;**36:**905–911.
26. Kumazawa M, Kohsaka T, Yamasaki M, Nakamura H, Kameyama Y. Effect of traumatic occlusion on periapical lesions in rats. *J Endod* 1995;**21:**372–375.
27. Bondevik O. Tissue changes in the rat molar periodontium following alteration of normal occlusal forces. *Eur J Orthod* 1984;**6:**205–212.
28. Nakamura Y, Noda K, Shimoda S *et al*. Time-lapse observation of rat periodontal ligament during function and tooth movement, using microcomputed tomography. *Eur J Orthod* 2008;**30:**320–326.
29. Kawakami T, Takise S, Fuchimoto T, Kawata H. Effects of masticatory movement on cranial bone mass and micromorphology of osteocytes and osteoblasts in developing rats. *Asia Pac J Clin Nutr* 2009;**18:**96–104.
30. Tanaka E, Sano R, Kawai N *et al*. Effect of food consistency on the degree of mineralization in the rat mandible. *Ann Biomed Eng* 2007;**35:**1617–1621.
31. ElDeeb ME, Andreasen JO. Histometric study of the effect of occlusal alteration on periodontal tissue healing after surgical injury. *Endod Dent Traumatol* 1991;**7:**158–163.
32. Kingsmill VJ, Boyde A, Davis GR, Howell PG, Rawlinson SC. Changes in bone mineral and matrix in response to a soft diet. *J Dent Res* 2010;**89:**510–514.
33. Bresin A, Kiliaridis S, Strid KG. Effect of masticatory function on the internal bone structure in the mandible of the growing rat. *Eur J Oral Sci* 1999;**107:**35–44.
34. Ho SP, Goodis H, Balooch M, Nonomura G, Marshall SJ, Marshall G. The effect of sample preparation technique on determination of structure and nanomechanical properties of human cementum hard tissue. *Biomaterials* 2004;**25:**4847–4857.
35. ASTM. *E 384-99: Standard Test Method for Microindentation Hardness of Materials*. West Conshohocken, PA: American Standard for Testing Materials International, 1999.
36. Thomas NR, Peyton SC. An electromyographic study of mastication in the freely-moving rat. *Arch Oral Biol* 1983;**28:**939–945.
37. Rippin JW. Collagen turnover in the periodontal ligament under normal and altered functional forces. II. Adult rat molars. *J Periodontal Res* 1978;**13:**149–154.
38. Rippin JW. Collagen turnover in the periodontal ligament under normal and altered functional forces. I. Young rat molars. *J Periodontal Res* 1976;**11:**101–107.
39. Kaneko S, Ohashi K, Soma K, Yanagishita M. Occlusal hypofunction causes changes of proteoglycan content in the rat periodontal ligament. *J Periodontal Res* 2001;**36:**9–17.
40. Amemiya A. An electron microscopic study on the effects of extraction of opposed teeth on the periodontal ligament in rats. *Jpn J Oral Biol* 1980;**22:**72–83.
41. Cohn SA. Disuse atrophy of the periodontium in mice following partial loss of function. *Arch Oral Biol* 1966;**11:**95–105.
42. Cohn SA. Disuse atrophy of the periodontium in mice. *Arch Oral Biol* 1965;**10:**909–919.
43. Gianelly AA. *Biologic Basis of Orthodontics*. Philadelphia: Lea & Febiger, 1971.
44. Inoue M. Histological studies on the root-cementum of the rat molars under hypofunctional condition. *J Jpn Prosthodont Soc* 1961;**5:**29–34.
45. Kinoshita Y, Tonooka K, Chiba M. The effect of hypofunction on the mechanical properties of the periodontium in the rat mandibular first molar. *Arch Oral Biol* 1982;**27:**881–885.
46. Koike K. The effects of loss and restoration of occlusal function on the periodontal tissues of rat molar teeth: histopathological and histometrical investigation. *J Jpn Soc Periodont* 1996;**38:**1–19.
47. Kronfeld R. Histologic study of the influence of function on the human periodontal membrane. *J Am Dent Assoc* 1931;**18:**1242–1274.
48. Saeki M. Experimental disuse atrophy and its repairing process in the periodontium of rat molar. *J Stomatol Soc Jpn* 1959;**26:** 317–347.
49. McCulloch CA, Lekic P, McKee MD. Role of physical forces in regulating the form and function of the periodontal ligament. *Periodontol 2000* 2000;**24:**56–72.
50. Berkovitz BKB, Moxham BJ, Newman HN. *The Periodontal Ligament in Health and Disease*, 1st edition. Oxford; New York: Pergamon Press, 1982:xiv, 470 p.
51. Robling AG, Castillo AB, Turner CH. Biomechanical and molecular regulation of bone remodeling. *Annu Rev Biomed Eng* 2006;**8:**455–498.
52. Robling AG, Turner CH. Mechanical signaling for bone modeling and remodeling. *Crit Rev Eukaryot Gene Expr* 2009;**19:**319–338.
53. Krishnan V, Davidovitch Z. On a path to unfolding the biological mechanisms of orthodontic tooth movement. *J Dent Res* 2009;**88:**597–608.
54. Junqueira LC, Bignolas G, Brentani RR. Picrosirius staining plus polarization microscopy, a specific method for collagen detection in tissue sections. *Histochem J* 1979;**11:**447–455.
55. Liu ZJ, Ikeda K, Harada S, Kasahara Y, Ito G. Functional properties of jaw and tongue muscles in rats fed a liquid diet after being weaned. *J Dent Res* 1998;**77:**366–376.
56. Holliday S, Schneider B, Galang MT *et al*. Bones, teeth, and genes: a genomic homage to Harry Sicher's "Axial Movement of Teeth". *World J Orthod* 2005;**6:**61–70.
57. Bondevik O. Tissue changes in the rat molar periodontium following application of intrusive forces. *Eur J Orthod* 1979;**2:**41–49.
58. Frost HM. *Bone Remodelling Dynamics*. Springfield, IL: Thomas, 1963:175.
59. Frost HM. *Bone Modeling and Skeletal Modeling Errors*. Springfield, IL: Thomas, 1973:ix, 214 p.
60. Frost HM. Obesity, and bone strength and "mass": a tutorial based on insights from a new paradigm. *Bone* 1997;**21:**211–214.
61. Jee WS, Frost HM. Skeletal adaptations during growth. *Triangle* 1992;**31:**77–88.
62. Roberts WE, Huja S, Roberts JA. Bone modeling: biomechanics, molecular mechanisms, and clinical perspectives. *Semin Orthod* 2004;**10:**123–161.
63. Ho SP, Kurylo MP, Fong TK *et al*. The biomechanical characteristics of the bone-periodontal ligament-cementum complex. *Biomaterials* 2010;**31:**6635–6646.
64. Balooch M, Habelitz S, Kinney JH, Marshall SJ, Marshall GW. Mechanical properties of mineralized collagen fibrils as influenced by demineralization. *J Struct Biol* 2008;**162:**404–410.
65. Landis WJ. A study of calcification in the leg tendons from the domestic turkey. *J Ultrastruct Mol Struct Res* 1986;**94:**217–238.
66. Gupta HS, Seto J, Wagermaier W, Zaslansky P, Boesecke P, Fratzl P. Cooperative deformation of mineral and collagen in bone at the nanoscale. *Proc Natl Acad Sci U S A* 2006;**103:**17741–17746.
67. Chattah NL. Design strategy of minipig molars using electronic speckle pattern interferometry: comparison of deformation under load between the tooth-mandible complex and the isolated tooth. *Adv Mater* 2008;**20:**1–6.